Journal of Hazardous Materials 403 (2021) 123875

Contents lists available at ScienceDirect

Journal of Hazardous Materials

journal homepage: www.elsevier.com/locate/jhazmat

Programmed responses of different life-stages of the seagrass *Ruppia sinensis* to copper and cadmium exposure

Ruiting Gu [a,b,c,d,1], Haiying Lin [e,1], Yi Zhou [a,b,c,d,f,*], Xiaoyue Song [g], Shaochun Xu [a,b,c,d], Shidong Yue [a,b,c,d], Yu Zhang [a,b,c,d], Shuai Xu [a,b,c,d], Xiaomei Zhang [a,b,c,f]

[a] CAS Key Laboratory of Marine Ecology and Environmental Sciences, Institute of Oceanology, Chinese Academy of Sciences, Qingdao 266071, China
[b] Laboratory for Marine Ecology and Environmental Science, Qingdao National Laboratory for Marine Science and Technology, Qingdao 266237, China
[c] Center for Ocean Mega-Science, Chinese Academy of Sciences, Qingdao 266071, China
[d] University of Chinese Academy of Sciences, Beijing 100049, China
[e] State Key Laboratory of Water Environment Simulation, School of Environment, Beijing Normal University, Beijing 100875, China
[f] CAS Engineering Laboratory for Marine Ranching, Institute of Oceanology, Chinese Academy of Sciences, Qingdao 266071, China
[g] Key Laboratory of Marine Ecosystem Dynamics, Second Institute of Oceanography, Ministry of Natural Resources, Hangzhou 310012, China

ARTICLE INFO

Editor: R. Debora

Keywords:
Ruppia
Copper
Cadmium
Different life stage
Subcellular accumulation
Transcription
Bioremediation

ABSTRACT

Seagrass meadows are recognized as crucial and are among the most vulnerable habitats worldwide. The aquatic plant genus *Ruppia* is tolerant of a wide salinity range, and high concentrations of trace metals. However, the tolerance of its early life stages to such trace metal exposure is unclear. Thus, the current study investigated the trace metal-absorbing capacity of three different life-history stages of *Ruppia sinensis*, a species that is widely distributed in China, by observing toxic symptoms at the individual, subcellular, and transcription levels. The seedling period was the most vulnerable, with visible toxic effects at the individual level in response to 50 μM copper and 500 μM cadmium after 4 days of exposure. The highest concentrations of trace metals occurred in the vacuoles and cytoplasmic structures of aboveground tissues. Genes related to signal identification and protein processing were significantly downregulated after 4 days of exposure to copper and cadmium. These results provide information relating to the strategies evolved by *R. sinensis* to absorb and isolate trace elements, and highlight the phytoremediation potential of this species.

1. Introduction

Trace elements resulting from increasing anthropogenic activities and discharged into aquatic environments pose ecological risks and threats to fishery populations, habitats, and the wider aquatic ecosystem (Cui et al., 2003; Cui et al., 2003). Mariculture is an important source of seafood, particularly for human consumption and, thus, the quality and safety aspects of these products are attracting increasing scientific and public attention (Perea-Juarez et al., 2016; Firth et al., 2019). Some vegetarian fish consume seagrass as their primary food source (Gillanders, 2007); therefore, the bioaccumulation of trace elements in seagrass may magnify the risk of contamination. Copper (Cu) and Cadmium (Cd) are two naturally occurring elements in the marine environment that have been shown to accumulate in crustaceans, such as shrimp (Greco et al., 2019; Liu et al., 2019). Both elements are derived naturally from crustal shale (Zhang et al., 2019), but they also originate from a variety of anthropogenic sources; e.g., impurities in phosphate fertilizers used in agricultural activities (Sabiha-Javied et al., 2009). A large quantity of trace metal waste from surrounding rivers has polluted the marine environment (Tian et al., 2020). In addition, port transportation may also cause, directly or indirectly, an increase in metal element pollution (Pan and Wang, 2012). Unlike organic pollutants, trace elements cannot be removed from aquatic ecosystems by natural processes (Roberts et al., 2008). However, quantifying the trace element content in water and sediments does not provide effective information about the biologically available or ecotoxicological relevance of these fractions (Chaphekar, 1991; Franzle, 2006). Therefore, a suitable biomonitor or bioaccumulator could provide a measure of element bioavailability, and act as a potential method for the removal of trace element contaminants from water and sediments.

* Corresponding author.
E-mail address: yizhou@qdio.ac.cn (Y. Zhou).
[1] Equal contribution to this work.

https://doi.org/10.1016/j.jhazmat.2020.123875
Received 15 February 2020; Received in revised form 30 August 2020; Accepted 31 August 2020
Available online 8 September 2020

Seagrass ecosystems provide critical ecological functions and services, such as recycling nutrients and providing food (Costanza et al., 1997; Fourqurean et al., 2012; Liu et al., 2013; Taylor et al., 2017; Unsworth et al., 2018; Duffy et al., 2019). However, seagrass meadows are disappearing at an alarming rate globally because of anthropogenic and natural disturbances (Orth et al., 2006; Waycott et al., 2009; Short et al., 2011; Maxwell et al., 2017; Jayathilake and Costello, 2018; Kendrick et al., 2019). Therefore, effective management and active restoration are important scientific topics worldwide (Zhou et al., 2014; Cullen-Unsworth and Unsworth, 2016; van Katwijk et al., 2016; Lefcheck et al., 2017; Jacob et al., 2018).

As a unique group of submerged marine angiosperms, seagrasses are the optimal trace element biomonitors of the marine environment (Martínez-Crego et al., 2008). Different species of seagrass vary in their effectiveness as bioindicators of different trace elements. In the natural seagrass populations of the Mediterranean sea, the Cu concentrations ranged from 0.25 –148 mg L^{-1} and 0.3–2 mg L^{-1} in *Posidonia oceanica* and *Zostera marina*, respectively, while the Cd concentrations were 0.09–44.0 mg L^{-1} and 0.5–2.5 mg L^{-1}, respectively. The levels were considered to be closely correlated with different environmental metal concentrations (Bonanno and Orlando-Bonaca, 2017). Moreover, different trace elements tend to accumulate in different seagrass tissues. In *Halophila stipulacea*, Cd accumulated in the order of leaves < rhizomes < roots, while Cu accumulated in the order of rhizomes < leaves < roots (Bonanno and Raccuia, 2018b). *Zostera* spp. showed different bioindicator capacities for Cu, Cd, Cr, Pb, and Zn among different species, with *Z. marina* having a higher metal enrichment capacity than *Z. japonica* and *Z. caespitosa* (Hu et al., 2019). However, these seagrasses grow in shallow marine and estuary environments, and rarely occur in mariculture ponds, in which there is a significant need for biomonitors to monitor trace elements.

Ruppia, a globally reported seagrass genus, can survive a range of salinity (e.g., 1.5–60 psu; Verhoeven, 1979). However, compared with other seagrasses, our understanding of the accumulation and biomonitoring capacity of trace elements in *Ruppia* is limited. Previous studies showed different absorption strategies applied among *Ruppia* spp (Kilminster, 2013; Malea et al., 2008; Sanchiz et al., 1999). The bioconcentration factors of Cu and Cd between *R. megacarpa* tissues and sediment were 3.3–3.4 and 7.6–9.1, respectively, indicating a powerful capacity to bioconcentrate trace elements (Kilminster, 2013). Moreover, almost 20 times the Cd concentration was found in *R. maritima* roots compared with the surrounding sediment, highlighting its high tolerance to Cd and suggesting its potential as a biomonitor (Malea et al., 2008). In China, the most widely distributed *Ruppia* species is *R. sinensis*, which is commonly found in mariculture ponds (Yu and den Hartog, 2014; Gu et al., 2019). There are few published data relating to how it accumulates trace elements and their resulting impact on the plant.

In plants, the uptake, translocation, sequestration, and detoxification of trace elements are vital processes that deal with excess amounts of metal elements (Shi et al., 2019). The seagrass responses to Cu and Cd have been investigated both in the laboratory and *in situ*. The exposure of adult *Thalassia hemprichii* to Cu and Cd results in leaf necrosis (Zheng et al., 2018). In *R. maritima*, leaf cell death was first detected in response to treatment with 88.95 μM Cd, which suggested that this species has a relatively high tolerance to this element (Malea et al., 2014). For subcellular distributions of trace elements in seagrasses, Cd mainly accumulates in soluble fractions in *P. oceanica* and *T. hemprichii* (Hamoutene et al., 1996; Feng et al., 2013), and there is evidence of Cd-induced DNA hypermethylation in *P. oceanica* (Greco et al., 2012). Previous research indicated that both Cu and Cd negatively impact seagrass through basic metabolism, such as photosynthesis and oxidation resistance (Lin et al., 2016; Greco et al., 2019). Moreover, phytochelatin-like peptides have been identified in leaves of *P. oceanica* and *T. testudinum* after exposure to Cd, indicating an active detoxification in seagrass (Greco et al., 2019). Those metabolic responses may be quickly revealed by transcript abundance in the different biosynthetic pathways.

Seed-based recruitment is considered to be the most effective and least costly to replant a new seagrass meadow (Marion and Orth, 2010; Reynolds et al., 2013; Xu et al., 2018). In recent decades, a growing number of researchers have investigated seed-based recruitment in seagrasses (Xu et al., 2016, 2018; Statton et al., 2017; Gu et al., 2018a; Yue et al., 2019). However, there is little information available relating to the tolerance and detoxification capacities of early life-stages of seagrasses in response to trace elements. Thus, the current study systematically explored the impacts of two trace elements (Cu and Cd) on three different *R. sinensis* life-history stages (dormant seeds, active seeds, and seedlings) to (i) observe any changes at the individual level in response to exposure to high Cu and Cd concentrations; (ii) to determine the subcellular accumulation of Cu and Cd in *R. sinensis* tissues; and (iii) to explore the toxic mechanisms and related biological pathways involved in the response to Cu and Cd based on transcriptome analyses.

2. Materials and methods

2.1. Sample collection

The Bohai and Yellow Seas are two semi enclosed epicontinental seas of the northwestern Pacific Ocean located in northeastern China, adjacent to the most developed areas in the country. The *R. sinensis* seeds used in this experiment were collected from two sites. Site 1 (40°28′1″ 122°17′53″) was an area of mariculture ponds in Yingkou City, Liaoning Province. Site 2 (37°24′16″ 122°19′47″) was an artificial wetland park in Weihai City, Shandong Province (Fig. 1). All seeds from the two sites were collected with reproductive shoots in September, 2017 (Site 1) and June, 2018 (Site 2). The shoots were then transferred to large containers of aerated seawater (salinity ~33 psu) and kept at room temperature (~20 °C) in darkness until the exocarps of the seeds decayed naturally and fell to the bottom. After culturing for 2 months, seeds with hard, black endocarps were sieved (0.7-mm meshes) and kept in low-temperature seawater (salinity 33 psu, 0 °C) before experimental use.

Overlying water, surface sediment, and *R. sinensis* shoots were collected from Site 3 in Dongying City (37°45′55.83″N, 118°58′13.03″E, Fig. 1), which is one of the biggest shrimp farming areas in northern China. All samples (each with three replicates) were brought back to the lab within 2 days. The overlying water was further filtered with a 0.22-μm sieve. The sediment samples were dried in an oven at 60 °C. The *R. sinensis* shoots were separated into above- and belowground tissues, which were then dried at 60 °C to a constant weight. Their Cu and Cd concentrations were determined at the analysis and testing center of the Institute of Oceanology, Chinese Academy of Sciences (Qingdao, China).

2.2. Seed germination period

Nondormant *R. sinensis* seeds with hard, black endocarps from Site 1 were used to explore the effects of Cu and Cd exposure on seed germination. Four Cu treatments (0, 0.5, 5, and 50 μM) and five Cd treatments (0, 0.5, 5, 50, and 500 μM) were established, each with six replicates. Cadmium and Cu were administered as $CdCl_2$ and $CuSO_4$, respectively. Each replicate contained 30 seeds placed in a 150-mL glass beaker. All treatments were cultivated with 5 psu artificial seawater (natural seawater diluted with distilled water), and placed in a light incubator with a light irradiance of 70 $\mu E \cdot m^{-2} \cdot s^{-1}$ in a 12-h photoperiod at 30 °C, which had previously been shown to be the optical germination conditions for *R. sinensis* seeds (Gu et al., 2018a). The seeds were exposed to either Cu or Cd for 14 days. The artificial seawater was changed every other day. In each treatment group, the final number of germinated seeds and the lengths of 30 seedlings were measured on Day 14. The seedlings were then collected and their above- and belowground tissues were washed three times with distilled water, dipped in 1 M EDTA solution for 5 min, and then washed again with distilled water. All samples were stored at –80 °C until further use.

For the trace element analysis, the samples were first dried in a freeze

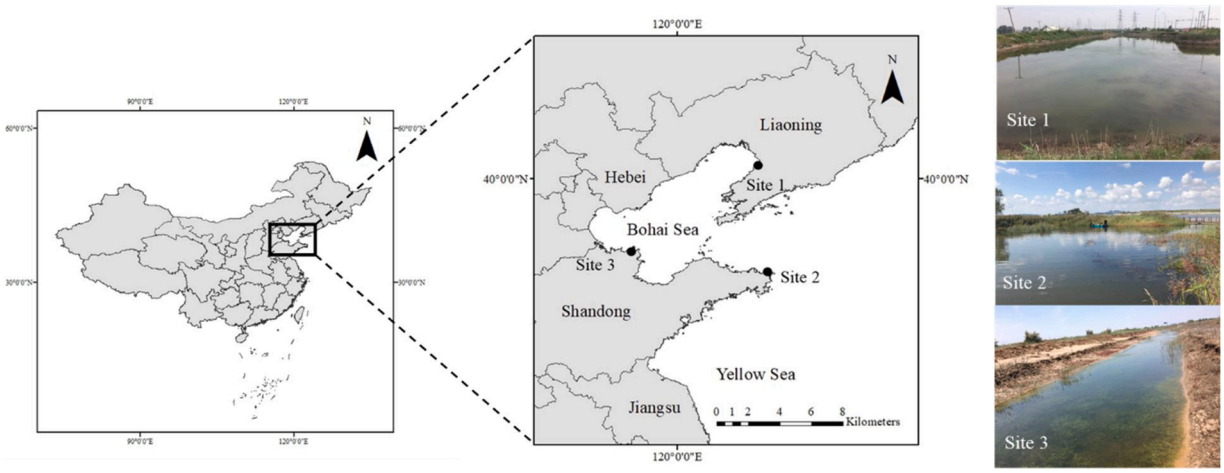

Fig. 1. Sample sites. Site 1 located in Yingkou City (Liaoning Province), Sites 2 and 3 were located in Weihai City and Dongying City, respectively (Shandong Province).

dryer (Martin Christ Alpha 1–2 LD plus Entry Freeze Dryer Package) for 48 h, then boiled at 160–220 °C in HNO_3 until nearly dry. The cooled residue was dissolved in 3 mL 1:1 HNO_3, and transferred with Milli-Q water to 14 mL of the total volume. The Cu and Cd concentrations were then determined using ICP-MS (Thermo Fisher, Icap-Qc, reference material GBW08517).

2.3. Seed dormancy period

Ruppia sinensis seeds are known to remain dormant at 0 °C (Gu et al., 2018a, b). Thus, the effects of Cu and Cd exposure on dormant *R. sinensis* seeds were explored by placing the seeds in a 0 °C incubator in continuous darkness (~400 seeds in 10 psu artificial seawater for every treatment) under continuous exposure to either Cd or Cu for 1 month. The seeds were then washed with distilled water five times. Half of the seeds (30 seeds from each replicate) were germinated in clean seawater under optimal germination conditions. Trace element treatments were as follows: controls; Cu (0.5, 5, 50, and 100 μM); and Cd (0.5, 5, 50, and 500 μM). The number of seeds germinated in each treatment group was recorded once they had been allowed to germinate for 14 days. The seedlings were then washed with both distilled water and EDTA solution as described earlier. All plant tissue samples and the remaining seeds (ungerminated and intact seeds) from each treatment group were then divided into three groups (aboveground tissues, belowground tissues, and seeds) and stored at –80 °C, until trace element concentration analysis, as described earlier.

2.4. Seedling period

Significant toxic effects of Cu and Cd were recorded on *R. sinensis* seedlings. Visible toxic effects only occurred following exposure to either 50 μM Cu or 500 μM Cd. To provide a more accurate description of the toxicity response of the seedlings, the seedling trace element exposure concentrations were reset to 100, 200, 400, and 600 μM Cd and 10, 20, 40, and 60 μM Cu. Healthy *R. sinensis* seeds were cultivated under optimal seed germination conditions, and healthy seedlings were selected once they had reached 4 ± 1 cm in height. Then, 20 seedlings were placed into a150-mL glass beaker, representing one replicate. Four replicates were designed for each treatment group. After 7 days, the shoot length of the seedlings in both the control and Cd treatment groups were measured, whereas the Chl-*a* content of the shoots in the control and Cu treatment groups was measured. Chl-*a* was analyzed fluorometrically according to the Welschmeyer method (Welschmeyer, 1994). Pigments were extracted with 90 % acetone (36 h in the dark at 4 °C; Tada et al., 2004). After centrifugation (3000 rpm, 15 min), the supernatant was used to determine the functional Chl-*a*.

The EC_{50} of Cu was based on the decreasing percentage of Chl-*a* content compared with the control treatment (Equation 1):

$$PD_i = \frac{C_0 - C_i}{C_0} \times 100\%, \quad (1)$$

where C_0 represents the average Chl-*a* concentration in control group, C_i represents the average Chl-*a* concentration in treatment group, and PD_i represents the decreasing percentage of Chl-*a* concentration after Cu exposure in different treatment.

By contrast, the EC_{50} of Cd was based on the percentage of shoot length inhibition after Cd exposure compared with the control group (Equation 2):

$$PI_i = \frac{L_0 - L_i}{L_0} \times 100\% \quad (2)$$

where L_0 represents the average shoot length in the control group, L_i represents the average shoot length in the treatment groups, and PI_i represents the percentage inhibition of shoot length after Cd exposure in the different treatment groups.

2.5. The accumulation and distribution of Cu and Cd in R. sinensis seedlings

The results of experiment 2.4 indicated an EC_{50} of Cu and Cd of 10 μM and 300 μM, respectively. Thus, investigations of the toxic effects of Cu and Cd on *R. sinensis* seedlings were based on these trace element concentrations.

The accumulation of Cu and Cd were investigated by analyzing seedling samples exposed to a trace element solution for different exposure times (0.5, 1, 2, 3, 4, 7, and 14 days). Healthy *R. sinensis* seedlings were cultivated as described in 2.4; 20 seedlings represented one replicate (with eight replicates for each exposure time for each trace element, giving a total of 112 replicates). When the seedlings reached 4 ± 1 cm in height, they were exposed to the trace element solution (10 psu artificial seawater, EC_{50} concentration of Cd or Cu) in 150-mL glass beakers, which were placed in a light incubator with a light irradiance of 70 $\mu E \cdot m^{-2} \cdot s^{-1}$ and a 12-h photoperiod at 30 °C. The water was refreshed every 2 days. Three replicates of aboveground and belowground tissues from each treatment group were analyzed as described earlier. The remaining aboveground tissues samples exposed for 12, 24, 48, or 96 h to the different Cu and Cd treatments were equally divided into three replicates and used to detect the subcellular distribution of the trace elements.

Aboveground samples were separated into four different subcellular fractions (cell wall and intact shoot tissues, chloroplast, mitochondria, and soluble fraction) by the gradient centrifugation technique as described by Wu et al. (2005) and Feng et al. (2013), with some modifications. Frozen aboveground tissues were homogenized in 4 mL precooled extraction buffer [50 mM Tris-HCl, 250 mM sucrose, 1.0 mM DTE (C4H10O2S2, Sigma D8255), 5.0 mM ascorbic acid and 1.0 % w:v Polyclar AT PVPP, pH 7.5] with a chilled mortar and pestle. The homogenates were divided into three replicates (every replication was 1 mL), and every replicate underwent three different centrifugations. First, the homogenate was centrifuged at 600 rpm for 10 min, resulting in a precipitate that contained mainly cell walls and tissue debris (F1). Then, 600 μL of the supernatant from each replicate was centrifuged at 1500 rpm for 10 min, resulting in a precipitate that contained mainly chloroplasts (F2). Lastly, the supernatant was centrifuged at 11,000 rpm for 35 min, resulting in a precipitate that contained mainly membranes and organelles (F3), whereas the resulting supernatant was considered to contain mainly vacuoles and cytoplasm (F4). All steps were performed at 4 °C and the fractions were stored at –20 °C for further trace element analysis, as described in 2.2.

The translocation factor (TF) was used to evaluate the ability of *R. sinensis* to transfer metals from belowground to aboveground tissues (Baker, 1981) (Eq. 3):

$$TF = \frac{M_{aboveground\ tissues}}{M_{belowground\ tissues}}, \quad (3)$$

where $M_{aboveground\ tissues}$ represents the average trace element concentration in aboveground tissues of *R. sinensis*; $M_{belowground\ tissues}$ represents the average trace element concentration in belowground tissues of *R. sinensis*. This index was applied to both the *R. sinensis* seedling exposure period and seed germination rate, for which the time of exposure and concentration of the trace element were considered main factors, respectively.

2.6. Transcriptomic profiling analysis

All *R. sinensis* seedlings used for transcriptomic profiling analysis were germinated in the same conditions described in 2.4. After 4 days of trace element exposure (Control, 10 μM Cu, and 300 μM Cd), the aboveground tissues from each treatment (with three replicates) were selected for Illumina sequencing (Allwegene Technology Inc., Beijing, China). Following harvest, tissues were immediately frozen in liquid nitrogen, and stored at –80 °C until use. The total RNA of each sample was extracted using an E.Z.N.A. Plant RNA Kit (OMEGA Bio-Tek, United States), following the manufacturer's protocol. After testing the RNA purity by Nanodrop and RNA fragment length test by Agilent 2100, and trimming adapter sequences and filtering low-quality reads, the clean reads were used to construct a new transcriptome using Trinity software (Grabherr et al., 2011).

The expected number of fragments per kb of transcript sequence per million bp sequenced (FPKM) was used as a unit to measure the gene expression levels (Trapnell et al., 2010). DESeq software was used to identify differentially expressed genes (DEGs) (Thomsen et al., 2010). Given that no genomic reference is available for *R. sinensis*, a transcriptomic reference was used for reads that were annotated based on seven public databases [NCBI Non-Redundant Protein Sequences (NR), NCBI Nucleotide Sequences (NT), Protein Family Dataset (PFAM), Eukaryotic Ortholog Groups (KOG), A manually annotated and reviewed protein sequence database (Swiss-Prot), Ortholog Database (KO), and Gene Ontology (GO)].

Kyoto Encyclopedia of Genes and Genomes (KEGG) pathway analyses were conducted, which considers each pathway as a unit to identify the major biochemical metabolic pathways and signal transduction pathways in which DEGs are involved (Kanehisa et al., 2008). The GO enrichment assignment analysis of DEGs was implemented using the GOseq R package based the Wallenius noncentral hypergeometric distribution (Young et al., 2010), which can adjust for gene length bias in DEGs (http://www.geneontology.org/).

SYBR Green I Real Time (RT)-PCR was used to exam the mRNA expression level of target genes. In total, seven genes (three replicates) were selected to amplify using primers that were designed through the PRIMER5 software. The calculations for determining the relative level of gene expression were made using the cycle threshold (C_T) value, according the $2^{-\triangle\triangle C_T}$ method (Livak and Schmittgen, 2001).

2.7. Statistical analysis

All data were statistically analyzed using SPSS 19. Copper and Cd concentrations in sediment, overlying water, and *R. sinensis* shoots *in situ* were analyzed with one-way ANOVA. All differences in seed germination, trace element accumulation, shoot growth inhibition, Chl-*a* reduction after different exposure doses and time were also compared with one-way ANOVA. Two-way ANOVA was used to compare the effects of trace element exposure time and trace element accumulation in the different subcellular fractions. The linear relationship and polynomial models were used to fit the Chl-*a* reduction data after Cu exposure and shoot growth inhibition data after Cd exposure, respectively. 'Dose–response' relationship models were applied for kinetic accumulations for both Cu and Cd. All graphs were generated by ArcMap 10.2, Excel 2016, and SigmaPlot 10.0.

3. Results

3.1. Trace elements concentration in environment and plants

The concentrations of both Cd and Cu in the environment and plants were as follows: [Sediment] > [Aboveground tissues] > [Belowground tissues] > [Overlying water] (Table 1). The environmental concentrations of Cu were one order of magnitude higher than those of Cd. The concentrations of Cu and Cd in the overlying water were 1/12 and 1/33 less than those in sediments, respectively, indicating more trace element contaminants accumulated in sediments. The concentrations of both trace elements were higher in aboveground tissues of *R. sinensis* than in their below-ground tissues (Table 1).

3.2. Individual responses to Cu and Cd exposure

One-way ANOVA showed that different Cu and Cd concentrations did not affect *R. sinensis* seed germination ($p_{Cu} = 0.226$, $p_{Cd} = 0.176$, Fig. 2; A, B). The most obvious impact of Cd was significant shoot growth inhibition following high dose exposure. Although a slight reduction in shoot length occurred following exposure to 50 μM Cd (5.6 mg L^{-1}), the most significant difference occurred in the 500 μM (56 mg L^{-1}) treatment group ($p < 0.001$, Fig. 2; C, D). The most visible toxic response to high concentrations of Cu was the yellowing of leaves after exposure to 50 μM (3.2 mg L^{-1}). The trace element concentrations in the above- and belowground tissues of these seedlings showed different correlational relationships (Fig. 2; E, F). For Cu exposure, more Cu accumulated in seedling tissues in the higher concentration exposure groups. However,

Table 1
Trace metal concentrations in overlying water, surface sediment, and above- and belowground tissues of *R. sinensis* (mean ± SE).

	Cu	Cd
Overlying water (μg·L^{-1})	1.24 ± 0.08^{d}	0.03 ± 0.01^{b}
Sediment (mg·kg^{-1})	15.13 ± 0.97^{a}	1.00 ± 0.38^{a}
R. sinensis		
Aboveground tissues (mg·kg^{-1})	9.44 ± 0.34^{b}	0.31 ± 0.08^{ab}
Belowground tissues (mg·kg^{-1})	6.70 ± 0.54^{c}	0.22 ± 0.05^{ab}

*Different letters (a, b, c and d) in the same column indicate significantly different trace metal concentrations.

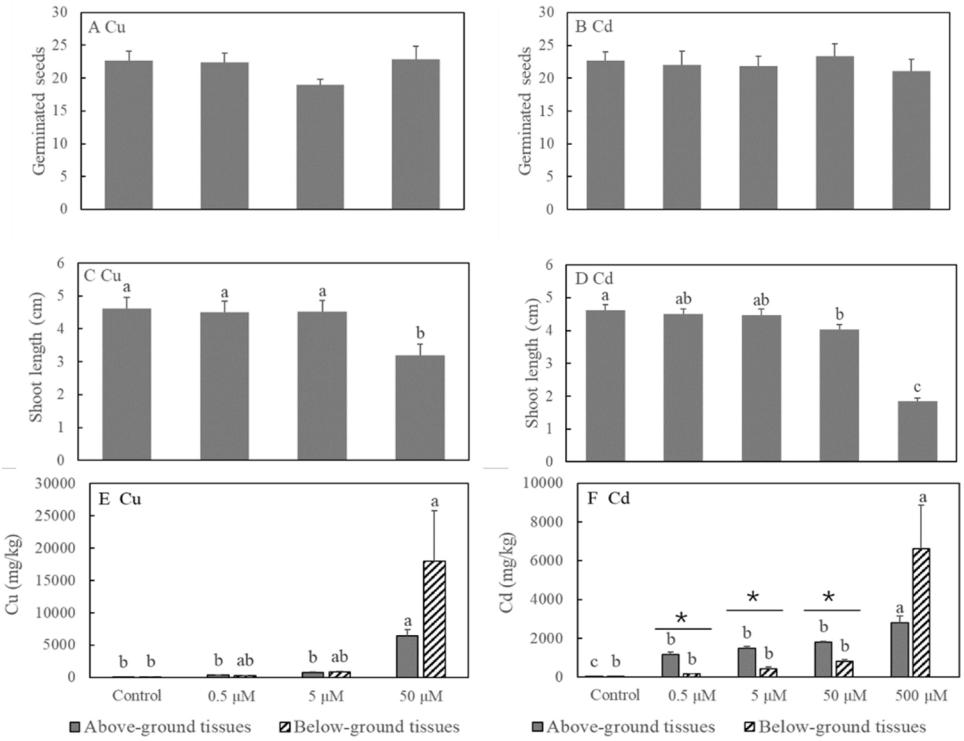

Fig. 2. *R. sinensis* seed germination, final shoot length, and trace metal accumulation in *R. sinensis* following different trace metal exposure conditions (Cu and Cd). Number of germinated *R. sinensis* seeds after exposure to different concentrations of (A) Cu and (B) Cd for 14 days. Final shoot lengths of *R. sinensis* after exposure to different concentrations of (C) Cu and (D) Cd for 14 days. Trace metal concentrations in aboveground and belowground tissues of *R. sinensis* seedlings following germination in different concentrations of (E) Cu and (F) Cd. Different letters indicated significant differences in different treatments; * indicates that the trace metal concentrations in the two different tissues were significantly different.

there were no significant differences in Cu accumulation between the above- and belowground tissues. By contrast, although, the trend in Cd accumulation was similar to that of Cu, more Cd accumulated in aboveground tissues compared with belowground tissues at relatively low Cd concentrations (0.5–50 μM), whereas no significant differences were found in either the control or high Cd concentration treatment groups.

There were no effects on germination of exposure of dormant seeds to either Cu or Cd for 1 month (Fig. 3; A, B). The Cu and Cd concentrations in all *R. sinensis* structures (seeds, and above-and belowground tissues) increased with increasing exposure concentration (Fig. 3; C, D). Exposure to 50 μM Cu resulted in ten times higher Cu accumulation in *R. sinensis* seeds compared with 5 μM Cu, whereas there was no significant difference between 50 μM and 100 μM Cu. The highest Cu accumulation occurred in belowground tissues at Cu concentrations < 50 μM; however, with increasing concentration exposure (100 μM), no significant differences in accumulation occurred between the two tissues. The Cd concentration in *R. sinensis* seeds increased in response to 50 and 500 μM Cd, being approximately nine times higher than at 5 μM Cd.

3.3. Accumulation kinetics of Cu and Cd in R. sinensis seedlings

For *R. sinensis* seedlings, acute toxicity occurred at ~50 μM Cu and ~500 μM Cd. Thus, the exposure trace element concentration ranges were reset to 10–60 μM Cu, and 100–600 μM Cd to explore the EC_{50} of Cu and Cd on *R. sinensis* seedlings. Chl-*a* reduction rate and seedling inhibition rate were used to represent the toxic effects following Cu and Cd exposure, respectively (Fig. S1). A polynomial model was used to fit the Chl-*a* reduction rate and Cu exposure concentration (Fig. S1; A, $y = -0.0544x^2 + 4.3515x + 12.245$, $R^2 = 0.8552$), and a linear relationship was found between Cd dose and seedling inhibition rate (Fig. S1; B, y =

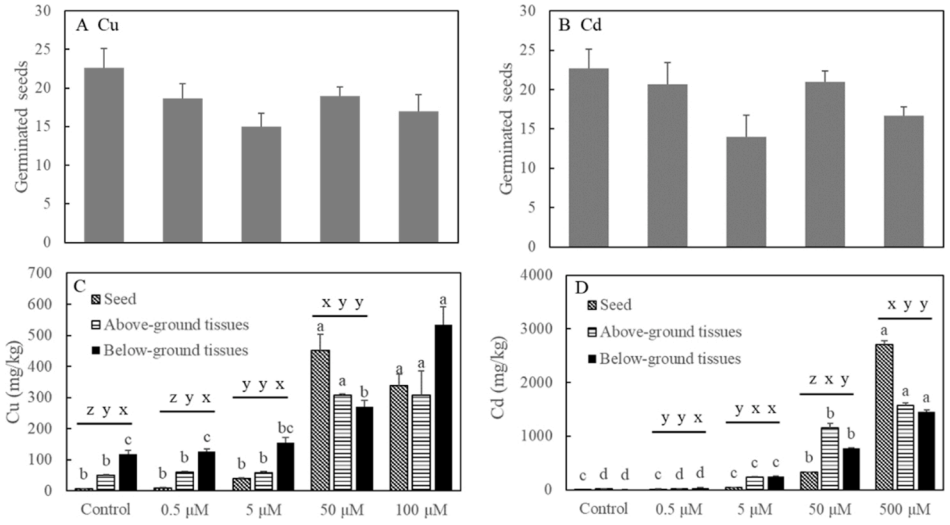

Fig. 3. Seed germination rates and absorbed doses of trace metal after exposure of dormant *R. sinensis* seeds to different trace metal concentrations. Number of germinated seeds after 1-month exposure of dormant seeds to (A) Cu and (B) Cd ($p_{Cu} = 0.102$; $p_{Cd} = 0.059$). Concentration of (C) Cu and (D) Cd in *R. sinensis* seeds and in above- and belowground tissues (mean ± SE). Different letters (x, y, and z) indicate significant differences among seeds and aboveground and belowground tissues at the same trace metal concentration. Different letters (a, b, c, and d) indicate significant differences in the same *R. sinensis* structures after exposure to different trace metal concentrations.

0.1724x – 0.949, $R^2 = 0.992$). The EC_{50} values of Cu and Cd were 9.9 μM and 295.5 μM, respectively.

The kinetics of Cu and Cd accumulation in *R. sinensis* seedlings were determined at 10 μM and 300 μM, respectively. Generally, the trace element concentrations in *R. sinensis* tissues significantly increased with the longer trace element exposure ($p_{Cu} < 0.001$, $p_{Cd} < 0.001$). After trace element exposure for 14 days, the Cu concentrations in above- and belowground tissues were 80 and 66 times higher than in the control treatments, respectively. Meanwhile, the Cd concentrations of above- and belowground tissues were 297 and 139 times higher than in the control treatments, respectively. Additionally, a sharply increase in both Cu and Cd concentration occurred during the first 4–7 days of exposure. Following Cu treatment, the changing trends and concentrations in above- and ground tissues were similar (Fig. 4; A, $R^2_{\text{aboveground tissues}} = 0.97$, $R^2_{\text{belowground tissues}} = 0.95$). By contrast, the sharp increase in Cd in aboveground tissues of *R. sinensis* seedlings was relatively delayed compared with that in belowground tissues (Fig. 4; B, $R^2_{\text{aboveground tissues}} = 0.96$, $R^2_{\text{belowground tissues}} = 0.98$). Moreover, after exposure for 14 days, the Cd concentration in aboveground tissues was higher than in the belowground tissues (Fig. 4B).

3.4. Subcellular response to Cu and Cd exposure

The Cu and Cd concentrations within the subcellular fractions (mitochondria, chloroplast, vacuoles, and cytoplasm) of the aboveground tissues were significantly impacted by exposure time ($p_{Cu} = 0.004$, $p_{Cd} < 0.001$, Fig. 5). In the control treatment group, there were no significant differences in Cu in different subcellular fractions ($p_{Cu} = 0.262$), whereas more Cd accumulated in mitochondria (~50 %, $p_{Cd} < 0.001$). After short-term trace element exposure, Cu and Cd concentrations showed significant variation among the different subcellular fractions, which were all higher than the corresponding control treatment. Overall, more trace elements accumulated in vacuoles and cytoplasm (F4), although the absolute values in all seedling subcellular fractions increased after exposure.

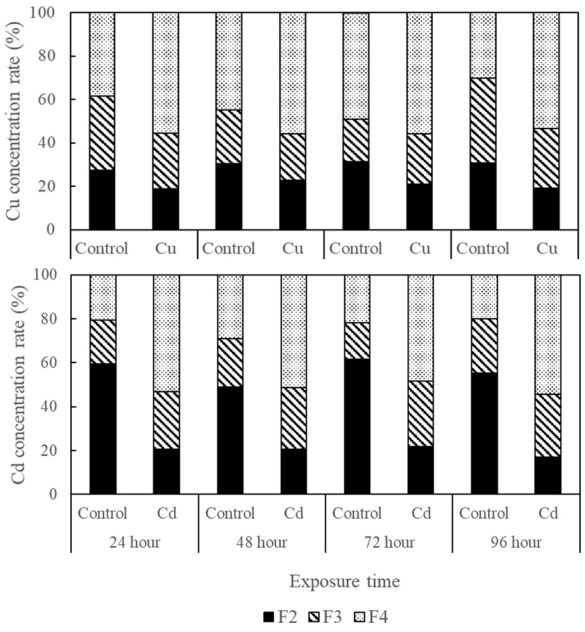

Fig. 5. Proportional distributions of Cu and Cd in different subcellular fractions after exposure of *R. sinensis* to Cu and Cd for different lengths of time. F2 mainly includes chloroplasts; F3 mainly comprises membranes and organelles; and F4 mainly includes vacuoles and cytoplasm.

We hypothesized that there would be no significant differences in trace element absorption rate between the *R. sinensis* seed germination period and seedling growth period. The results showed a higher TF at higher trace element concentrations (> 1); in the EC_{50} treatments (50 μM Cu and 500 μM Cd), the TF of both trace elements was < 0.5.

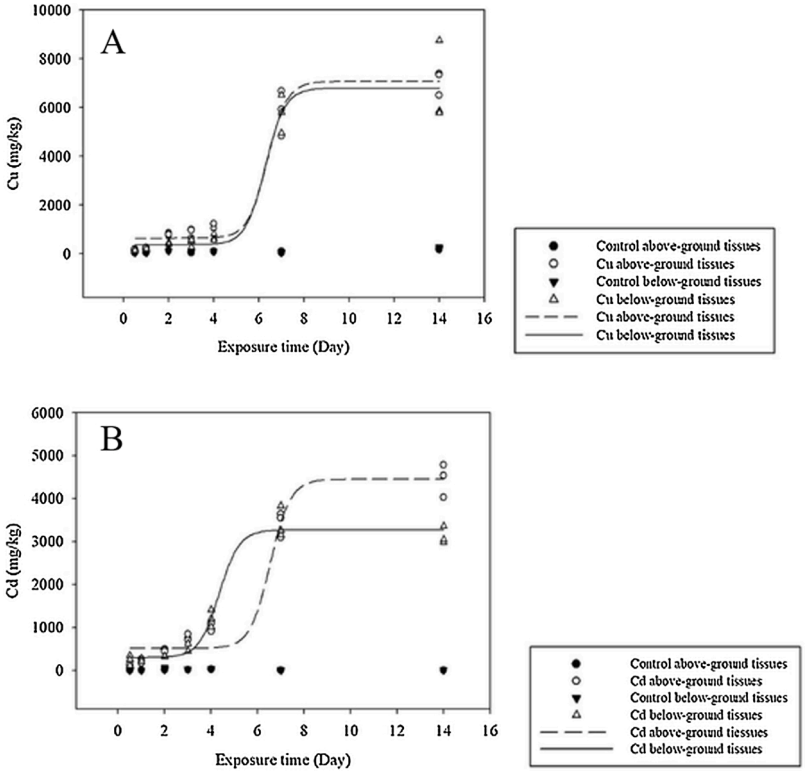

Fig. 4. Relationships between trace metal exposure time and trace metal concentration in above- and belowground tissues of *R. sinensis* seedlings. Relationships between (A) Cu exposure time and concentration and (B) Cd exposure time and concentration in *R. sinensis* seedling tissues.

However, the exposure time was not the main factor influencing TF, given that nearly all the TFs in the 10-μM Cu exposure groups were > 1 regardless of the exposure time. By contrast, the TFs in the 300-μM Cd treatment groups were all < 0.5 (Table 2).

3.5. Molecular response to Cu and Cd exposure

After sequencing, 309 660 289 raw read pairs were produced, resulting in 96.8 % clean reads (Table S1). The range of transcripts produced from the clean reads was from 201–14 132 bp, with an average of 334 bp. By taking the longest transcript of each gene as a unigene, 422 650 unigenes were identified, with an average size of 291 bp. Based on the SwissProt, NR, NT, KO, PFAM, GO, and KOG databases, the sequences were successfully annotated: 143,187 unigenes (33.88 %) in NR and 148,470 unigenes (35.13 %) in Pfam; 205,149 unigenes (48.54 %) were annotated in at least one database. Gene expression levels were estimated using RSEM (Li and Dewey, 2011) for each sample. A full comparison of the DEGs for each treatment and a full list of DEG levels and the associated FPKM density distributions for each treatment are shown in Fig. S2.

Fig. S3 shows the number of common and unique DEGs among the different trace element exposure groups. For the Cu versus Cd exposure treatments, 8891 (82.3 %) and 46 (2.3 %) genes were differentially expressed ($p_{adj} < 0.05$), respectively, whereas 1915 genes were common to both treatments. The differentially expressed genes after Cu and Cd exposure were illustrated using volcano diagrams (Fig. S3; B, C). After eliminating the effects of biological mutation ($p_{adj} < 0.05$), 10,806 genes (3.5 % upregulated and 96.5 % downregulated) and 1961 genes (2.2 % upregulated and 97.8 % downregulated) were observed in the Cd and Cu treatment groups, respectively. There were more downregulated genes in both treatment groups, indicating that gene silencing and/or downregulation is a common feature after Cu and Cd exposure.

To further understand the DEG function, KEGG enrichment was performed. Three and seven KEGG pathways were considered significantly downregulated after Cd and Cu exposure, respectively (corrected *p*-value < 0.05, Table 3). Moreover, 'RNA transport' was the only downregulated KEGG pathway common to both trace element exposure treatments. GO enrichment analyses were applied to further identify the DEG sets. In both the Cu and Cd treatment groups, the most DEGs were enriched in 'cellular components', followed by 'biological process' and 'molecular function' (Fig. 6). Similar subclassifications in 'biological process', 'cellular components', and 'molecular function' were downregulated following Cd and Cu exposure, with 'protein metabolic process' being the most common GO term. DEGs related to 'signal transduction and signal pathway', 'ion transport', and 'photosynthesis' were found significantly downregulated in the Cd treatment groups, whereas DEGs related to 'macromolecule biosynthetic and metabolic process' and 'response to oxidative stress' were found downregulated in the Cu treatment groups. 'Lipid transport' and 'lipid localization' were the only two biological processes significantly upregulated in the Cu treatment groups. 'Ribosome' and 'intracellular organelle and cytoplasmic part' were the common cellular components impacted following either Cd or Cu exposure. 'Mitochondrial part including its envelope and membrane', 'actin cytoskeleton', and 'myosin complex' were the specific cellular components influenced by Cd (Tables S2 and S3). 'GTP binding', 'guanyl nucleotide' and 'ribonucleotide binding and some protein binding' were common to both Cd and Cu treatment groups; however, some trace element ion binding, such as zinc ion binding, was only found in the Cd treatment groups. By contrast, the molecular functions of ATPase activity and antioxidant activity and their related genes were regulated in the Cu treatment groups.

Table 2
Translocation factors of Cu and Cd in above- and belowground tissues of *R. sinensis* after different lengths of exposure to Cu and Cd.

Trace element	concentration (μM)	exposure time (Day)	TF
R. sinensis seed germination period			
Cu	0.5	14	1.20
	5	14	0.86
	50	14	0.36
Cd	0.5	14	3.73
	5	14	1.73
	50	14	2.20
	500	14	0.42
R. sinensis seedling exposure period			
Cu	10	0.5	0.97
	10	1	1.27
	10	2	1.84
	10	3	1.81
	10	4	1.69
	10	7	1.10
	10	14	1.02
Cd	300	0.5	0.42
	300	1	0.37
	300	2	0.41
	300	3	0.41
	300	4	0.34
	300	7	0.34
	300	14	0.31

Table 3
Significantly downregulated genes and their KEGG enrichment pathways after exposure of *R. sinensis* to Cu and Cd for 4 days.

ID	Term	Input number	Background number	Corrected *P*-Value
Cd & Control_down				
osa04141	Protein processing in endoplasmic reticulum	174	189	0.027
osa04144	Endocytosis	121	127	0.039
osa03013	RNA transport	137	149	0.039
Cu & Control_down				
osa03010	Ribosome	207	337	< 0.001
osa04145	Phagosome	34	77	< 0.001
osa00910	Nitrogen metabolism	18	28	< 0.001
osa00190	Oxidative phosphorylation	39	137	< 0.001
osa03013	RNA transport	37	149	0.002
osa00630	Glyoxylate and dicarboxylate metabolism	20	63	0.005
osa03050	Proteasome	18	63	0.021

Input number represents the number of relatively differentially expressed genes (DEGs) in the pathway; background number represents the total relative gene number in the pathway; corrected *P*-value represents the statistical *P*-value after adjustment; it was considered an enrichment pathway when the corrected *p*-value was < 0.05.

4. Discussion

Here, we investigated the Cu and Cd toxicity and detoxification mechanisms at the individual, cellular, and molecular levels in *R. sinensis*. The results not only serve as a general demonstration of the potential of this species as a bioindicator for use in its habitats and mariculture ponds, but also provide reference data for managing and utilizing *R. sinensis* in a bioindicator capacity.

4.1. Metal tolerance and toxic effects in individual R. sinensis

Copper and Cd are essential and nonessential elements in seagrasses, respectively, but can result in toxic effects above certain threshold concentrations and even at very low levels (Lin et al., 2016, 2018; Bonanno and Di Martino, 2017; Sanchez-Quiles et al., 2017). Different tolerances to Cu and Cd have been reported in different seagrasses species. For example, *T. hemprochii* experienced ~50 % leaf necrosis after exposure to 0.1 mg L^{-1} Cu^{2+} for 5 days (Zheng et al., 2018), whereas *Zostera* spp. showed toxic effects at Cu concentrations < 20 μg g^{-1} (Hu et al., 2019). The quantum yield declined rapidly when *H. ovalis*

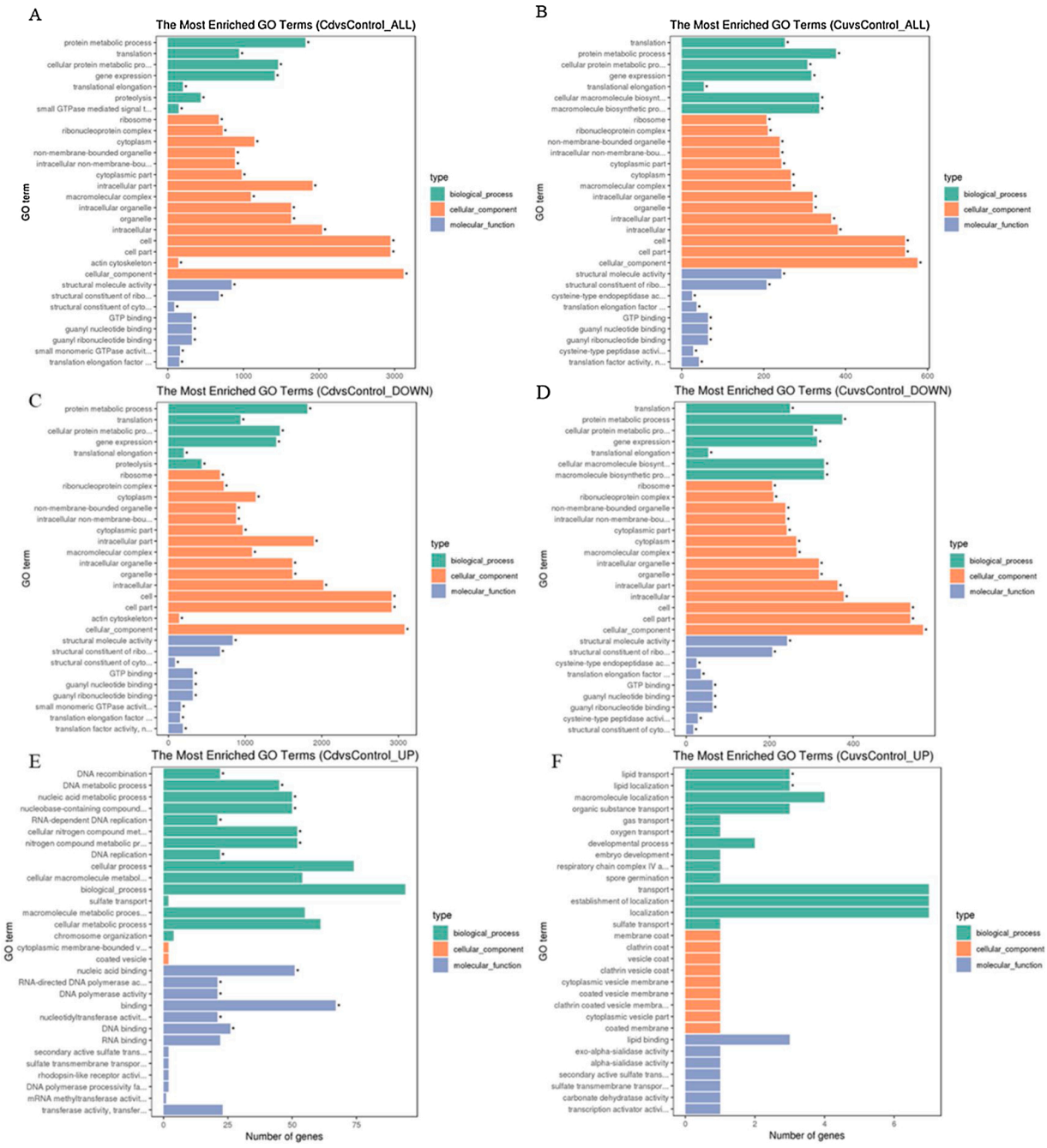

Fig. 6. Bar graphs of three major gene ontology (GO) terms for differentially expressed genes following the exposure of *R. sinensis* to Cu and Cd. The most-enriched GO terms following (A) Cd exposure and (B) Cu exposure compared with the control treatment. The most downregulated enriched GO terms following (C) Cd exposure and (D) Cu exposure compared with the control treatment. The most upregulated enriched GO terms following (E) Cd exposure and (F) Cu exposure compared with the control treatment; * indicates significantly enrichment, *padj* < 0.005.

was exposed to 1 mg L^{-1} Cd (Ralph and Burchett, 1998). By contrast, *R. sinensis* showed higher tolerance to both Cu and Cd, with the main morphological toxic effects being yellowing of leaves and inhibition of seedling elongation, respectively. However, these visible toxic effects only occurred when *R. sinensis* seedlings were exposed to relatively high Cu and Cd concentrations (~50 μM and ~500 μM, respectively). Moreover, Cu was shown to be more toxic to *R. sinensis* seedlings compared with the nonessential Cd. These differences could be explained by the active uptake mechanisms for essential elements (i.e., Cu), whereas tolerance strategies are involved for nonessential metals (i.e., Cd) (Ralph and Burchett, 1998).

The laboratory experiment revealed positive correlations between the trace element concentrations in seedling tissues and water (Fig. 2). Moreover, compared with the water column, higher concentrations of Cu and Cd were found in sediments (Table 1), which is considered to be a sink for trace elements (Bonanno and Raccuia, 2018b; Zheng et al., 2018). Although previous studies indicated that seagrasses, such as *H. stipulacea* and *Z. marina*, could absorb Cd from the water column via their leaves, rooted submerged plants primarily extract elements from the sediment (Lyngby and Brix, 1982; Bonanno and Raccuia, 2018b). Thus, the 'sediment–root' pathway may also be the main uptake route for natural *Ruppia* populations. Translocation factors suggest that the trace element translocation capacity in seagrass tissues is >1 in three *Zostera* seagrasses, which exhibited strong translocation processes

between their above- and belowground tissues (Hu et al., 2019). The TF values in *R. sinensis* seedlings decreased with increasing Cu exposure concentrations. Moreover, TF values were < 1 when exposed to Cd < 300 μM, but were > 1 when exposed to 500 μM Cd (Table 2). The Cu and Cd kinetics accumulation model of *R. sinensis* seedlings showed two relative stable trace element accumulation stages (exposure <4 days or > 7 days), when more trace elements accumulated in aboveground tissues than in belowground tissues (Fig. 4). These results indicated that a resistance mechanism existed in the early trace element-exposure period, which protected *Ruppia* from trace metal toxicity. However, with the extension of exposure time, the metal toxicity overrode this resistance mechanism, resulting in a quicker absorption and accumulation of trace elements in *Ruppia* tissues.

Significant variations in Cu and Cd accumulation were shown in the different *R. sinensis* life-history stages. Although the germination rate of dormant and active *R. sinensis* seeds exposed to high concentrations of Cu and Cd (100 μM and 500 μM, respectively) was not affected, the accumulated concentration of Cu and Cd was as follows: seed dormancy < seed germination ~ seedling. This indicated that dormant seeds have a poor trace element-absorbing ability and that endocarps might be an important protection against exposure to low concentrations of trace elements. These results also indicate that a low concentration metal sulfate treatment could be used to inhibit bacterial growth during long-term storage of *R. sinensis* seeds, as was used with *Z. marina* seeds (Figs. 2E, F, 3 C, D, and 4) (Govers et al., 2017). Exposing active seeds to different concentrations of Cd and Cu resulted in no significant variations in the accumulated concentration between different vegetative tissues, although more Cd accumulated in aboveground tissues under relatively low Cd treatments (0.5–50 μM) (Fig. 2; E, F). Moreover, higher levels of Cu and Cd in *R. sinensis* aboveground tissues suggest that these tissues would be more sensitive trace element biomonitors.

4.2. Trace element resistance strategies of R. sinensis

There are two possible trace element tolerance strategies adopted by seagrasses: a compartmentalization or exclusion strategy, which favors the accumulation of elements in belowground tissues (e.g., roots); and a removal strategy, whereby most absorbed elements accumulate in aboveground tissues (e.g. leaves) (Bonanno and Di Martino, 2017; Bonanno and Raccuia, 2018a). Based on the kinetics of Cu and Cd accumulation in *R. sinensis* tissues in the current study, three accumulation steps occurred with increasing exposure time: (i) slow increase; (ii) sharp increase; and (iii) relative steady. The relatively slowly increasing trace element accumulation during *R. sinensis* seedling exposure for < 4 days suggested strong physiological resistance during the early stage of trace element exposure (Fig. 4). Thus, an additional tolerance mechanism investigation focused on this first resistance period (i.e., exposure Cu and Cd for < 4 days).

Copper is an essential element that not only acts as structural element involved in the electron transport of chloroplasts and mitochondria, but it also serves as a cofactor in enzymes, such as Cu/Zn superoxide dismutase (Yruela, 2005). Thus, the Cu subcellular distribution in *R. sinensis* leaf cells suggests relatively high concentration in vacuoles, cytoplasm, and chloroplasts in the natural state (Fig. 5: Control treatment). However, Cd, which is considered a non-essential element, accumulated in F2 (chloroplasts) after exposure to extremely low concentrations, suggesting that the chloroplasts are sensitive to Cd (Fig. 5: Control treatment). Additionally, the chloroplast structure may become disorganized, forming misshaped envelopes and unclear thylakoids, as well as having numerous large and bright starch granules as reported in terrestrial plants *Oryza sativa* L. (Liu et al., 2020). The subcellular fraction, 'cell wall', is considered to be the first barrier to the entry of trace elements into cells (Fu et al., 2011; Gallego et al., 2012; Wang et al., 2016). After trace elements enter the cell, the vacuoles, which comprise 90 % of the total cell volume, are the main trace element storage sites (Chen et al., 2005; Pittman, 2005; Sharma et al., 2016). Compared with the control treatment, the accumulation rates of Cu and Cd in vacuoles and cytoplasm of *R. sinensis* seedlings obviously increased after exposure to EC_{50} concentrations (Fig. 5), indicating that a large proportion of invasive trace elements were held at these locations, and that vacuoles and cytoplasm were attempting to perform their functions of protecting plant cells from damage by trace elements, compartmentalizing organic acids, proteins, and bases and chelating the metal ions (Clemens et al., 2002).

4.3. Molecular responses of R. sinensis after trace element exposure

Randomly selected genes in the KEGG enrichment pathways were further analyzed using RT-qPCR (Table S4). All the genes were significantly downregulated compared with the control treatment group, which confirmed that the RNA-seq method generated reliable expression data. Both Cu and Cd stresses activate biochemical defenses that result in reprogramming of the *R. sinensis* seedling transcriptome. Although Cd accumulation resulted in more DEGs, more KEGG enrichment pathways in the Cu exposure treatment groups were significantly reprogrammed (Fig. 6 and Table 3). This might also be the result of the higher toxicity resulting from Cu accumulation compared with Cd. In general, ribosomes and cytoplasm were the two main structures impacted by Cu and Cd (Fig. 6, Tables S2 and S3). The regulation and processing of proteins, signaling, and intracellular components were the most commonly impacted biological processes after exposure to Cu and Cd for <4 days (Fig. 6, Tables S2 and S3). Interestingly, in the Cu-exposure treatment, the levels of Chl-*a* significantly decreased after 7 days, while no statistically significant differences in the expression levels of any photosystem members were identified after 4 days (Fig. 6 and S1). Similar results were found in *Z. muelleri* at 7 days after exposure to 0.25 and 0.5 mg L^{-1} Cu (Buapet et al., 2019; Mohammadi et al., 2019). However, the transcriptomes of *Z. japonica* associated with photosynthetic pathways were significantly regulated under the higher exposure concentration (3.2 mg L^{-1} Cu) for the same exposure time (Lin et al., 2018). Compared with acute toxicity, the chronic toxicity was always exhibited in relation to the low exposure concentration and a longer exposure time. On the basis of the kinetics of the Cu-accumulation curve in *R. sinensis*, a sharp increase after approximately 6 days of exposure might explain the role of the longer exposure time in damaging shoot physiology, including the photosynthetic pathways (Fig. 4).

Unlike impacts on RNA in some terrestrial plants (He et al., 2013), Cd mainly impacted the DNA recombination and metabolic processes of *R. sinensis* seedlings during the early stages of Cd exposure. Genes related to DNA and the nucleolus were significantly upregulated (Table S2). These changes could result in morphological modifications to the nucleoli and related metabolic activity changes (Huybrechts et al., 2019). The actin cytoskeleton has an essential role in biological processes in plants, such as cell division, cell expansion, and the establishment of polar cell growth (Paez-Garcia et al., 2018). The downregulated genes of the actin cytoskeleton could reflect the reduced plant growth that occurred during early Cd exposure, given its role in the growth and development of plants (Qin and Dong, 2015). Sequestration of Cd-chelates in vacuoles is an important pathway to reduce the toxic effects of Cd (Lux et al., 2011). Several genes related to binding were upregulated after Cd exposure, whereas genes associated with GTP and nucleic acid binding were downregulated (Table S3); this suggests that Cd detoxification occurs by activating antioxidative enzymes and glutathione (GSH) synthesis through the formation of Cd-ligands to reduced GSH and phytochelatins, as reported for *Z. marina* (Conn and Gilliham, 2010; Park et al., 2012; Greco et al., 2019). Moreover, metallothionein and nicotianamine are also metal chelators that can be induced by Cu and Cd exposure, and have important roles in metal transition and detoxification (Zimeri et al., 2005; Cornu et al., 2015).

The common physiological toxic effects of Cu include disruption of photosystem II (Barón et al., 1995), the loss of biological membrane integrity, lipid peroxidation, and protein and DNA damage (Körpe and

Aras, 2011; Thounaojam et al., 2012). Compared with Cd, the early toxic effects of Cu exposure resulted in the upregulation of genes related to lipids, which are a vital component of cell membranes (Table S3; Lodish et al., 2000). Moreover, the downregulated genes related to macromolecules might indicate that Cu exerts toxic effects via protein dysfunction and promotion of oxidative stress (Buapet et al., 2019). Heat shock proteins, which have important roles in seagrass adaptability and resilience when faced with heat stress, are also significantly downregulated after Cd exposure (Franssen et al., 2014). There is also evidence of Cd-induced DNA hypermethylation in *P. oceanica* (Greco et al., 2012). Although both Cu and Cd induce the overexpression of DNA methyltransferases (Greco et al., 2019), no significant changes related to DNA hypermethylation were recorded during the early stages of trace element exposure (Table S2 and S3).

4.4. Potential biomonitor and phytoremediation species

Seagrasses have previously been used as biomonitors to assess spatial contamination because of their trace element accumulation capacity, tolerance level, and bioindication potential (Bonanno and Orlando-Bonaca, 2017). Like other seagrass species, the trace element concentrations in *R. sinensis* tissues also reflected the trace element levels in the surrounding environment. Consequently, they can also serve as potential biomonitors for trace element containment in coastal ecosystems. The strong tolerance to high concentrations of metal elements in their plant tissues indicates that seagrasses, through phytoextraction, may act as bioremediation agents for metal contaminated areas (Nouri et al., 2009). *Z. marina* accumulated greater concentrations of Cu and Cd in aboveground tissues, which may facilitate the removal of metal elements owing to the high turnover rate of leaves (Lee et al., 2019). Moreover, the large amounts of *Z. marina* leaf detritus would form large litter banks that could be cleaned up or removed to the waste disposal sites rather than enter the marine food web (Lee et al., 2006; Achamlale et al., 2009; Cebrian, 2002). Like *Z. marina*, the high environmental adaption capability and growth rate (Gu et al., 2018b, 2019) as well as the high tolerance to trace elements, suggests that *R. sinensis* has the potential to act as a bioremediator.

5. Conclusion

The seedling stage was the most vulnerable in terms of the effects of exposure to Cd and Cu. Although the different growth stages had different Cu and Cd absorbing capacities, extremely high Cu and Cd concentrations (~50 μM and ~500 μM, respectively) resulted in visible toxicity symptoms in *R. sinensis* seedlings. The results also revealed the accumulation of Cd and Cu in the vacuoles and cytoplasm of the aboveground tissues. The toxic effects of Cu and Cd on *R. sinensis* seedlings were shown on occur during the early stages of exposure, via transcriptome analysis. Genes related to membrane, intracellular and cytoplasmic components were significantly impacted after Cd exposure, whereas genes related to signal identification and cellular components that act as hubs for energy transport, such as mitochondria, actin cytoskeleton, and the myosin complex, were downregulated after Cd exposure. These transcriptomic results could explain the inhibition of *R. sinensis* seedling growth in the Cd treatment groups. *Ruppia sinensis* is a high Cu- and Cd-tolerant seagrass that is not only a suitable bioindicator, but also has potential in phytoremediation. However, more research is required to fully determine the toxic effects of Cu and Cd on *R. sinensis*, the related detoxification mechanisms, and the interactions between the accumulation and the toxicity of the two trace elements, before this species can be used effectively as a biomonitoring and phytoremediation tool.

CRediT authorship contribution statement

Ruiting Gu: Conceptualization, Investigation, Methodology, Writing - original draft. **Haiying Lin:** Conceptualization, Writing - review & editing. **Yi Zhou:** Supervision, Funding acquisition, Writing - review & editing. **Xiaoyue Song:** Investigation. **Shaochun Xu:** Investigation. **Shidong Yue:** Investigation. **Yu Zhang:** Investigation. **Shuai Xu:** Investigation. **Xiaomei Zhang:** Investigation.

Declaration of Competing Interest

The authors declare that they have no known competing financial interests or personal relationships that could have appeared to influence the work reported in this paper.

Acknowledgements

We would like to thank Kai Xiao and Gang Li for their help with the field survey, Jingchun Sun, Cong Yu, Meijun Liu, and Chuang Li for their assistance during the laboratory experiments, and Yao Liu from the Public Tech-Supporting Center of IOCAS for the ICP-MS analysis. This research was supported by the National Key R&D Program of China (2019YFD0901301/2018YFC1406404), the Key Research Project of Frontier Sciences of CAS (QYZDB-SSW-DQC041-1), the National Science & Technology Basic Work Program (2015FY110600), the Key Research and Development Program of Shandong Province (2017GHY15111), and the Taishan Scholars Program (Distinguished Taishan Scholars).

Appendix A. Supplementary data

Supplementary material related to this article can be found, in the online version, at doi:https://doi.org/10.1016/j.jhazmat.2020.123875.

References

Achamlale, S., Rezzonico, B., Grignon-Dubois, M., 2009. Evaluation of *Zostera* detritus as a potential new source of zosteric acid. J. Appl. Phycol. 21, 347–352.
Baker, A.J.M., 1981. Accumulators and excluders - strategies in the response of plants to heavy metals. J. Plant Nutr. 3, 643–654.
Barón, M., Arellano, J.B., Gorgé, J.L., 1995. Copper and photosystem II: a controversial relationship. Physiol. Plantarum 94, 174–180.
Bonanno, G., Di Martino, V., 2017. Trace element compartmentation in the seagrass *Posidonia oceanica* and biomonitoring applications. Mar. Pollut. Bull. 116, 196–203.
Bonanno, G., Orlando-Bonaca, M., 2017. Trace elements in Mediterranean seagrasses: accumulation, tolerance and biomonitoring. A review. Mar. Pollut. Bull. 125, 8–18.
Bonanno, G., Raccuia, S.A., 2018a. Comparative assessment of trace element accumulation and bioindication in seagrasses *Posidonia oceanica*, *Cymodocea nodosa* and *Halophila stipulacea*. Mar. Pollut. Bull. 131, 260–266.
Bonanno, G., Raccuia, S.A., 2018. Seagrass *Halophila stipulacea*: capacity of accumulation and biomonitoring of trace elements. Sci. Total Environ. 633, 257–263.
Buapet, P., Mohammadi, N.S., Pernice, M., Kumar, M., Kuzhiumparambil, U., Ralph, P.J., 2019. Excess copper promotes photoinhibition and modulates the expression of antioxidant-related genes in *Zostera muelleri*. Aquat. Toxicol. 207, 91–100.
Cebrian, J., 2002. Variability and control of carbon consumption, export, and accumulation in marine communities. Limnol. Oceanogr. 47, 11–22.
Chaphekar, S.B., 1991. An overview on bio-indicators. J. Environ. Biol. 12, 163–168.
Chen, T.B., Yan, X.L., Liao, X.Y., Xiao, X.Y., Huang, Z.C., Xie, H., Zhai, L.M., 2005. Subcellular distribution and compartmentalization of arsenic in *Pteris vittata* L. Chin. Sci. Bull. 50, 2843–2849.
Clemens, S., Palmgren, M.G., Kramer, U., 2002. A long way ahead: understanding and engineering plant metal accumulation. Trends Plant Sci. 7, 309–315.
Conn, S., Gilliham, M., 2010. Comparative physiology of elemental distributions in plants. Ann. Bot.-Lond. 105, 1081–1102.
Cornu, J.Y., Deinlein, U., Horeth, S., Braun, M., Schmidt, H., Weber, M., Persson, D.P., Husted, S., Schjoerring, J.K., Clemens, S., 2015. Contrasting effects of nicotianamine synthase knockdown on zinc and nickel tolerance and accumulation in the zinc/cadmium hyperaccumulator *Arabidopsis halleri*. New Phytol. 206, 738–750.
Costanza, R., d'Arge, R., de Groot, R., Farber, S., Grasso, M., Hannon, B., Limburg, K., Naeem, S., O'Neill, R.V., Paruelo, J., Raskin, R.G., Sutton, P., van den Belt, M., 1997. The value of the world's ecosystem services and natural capital. Nature 387, 253–260.
Cui, Y., Ma, S., Li, Y., Wang, M., Xin, F., Chen, J., 2003. Pollution situation in the Laizhou Bay and its effects on fishery resources. Mar. Fish. Res. 24 (1), 35–41 (In Chinese).
Cullen-Unsworth, L.C., Unsworth, R.K.F., 2016. Strategies to enhance the resilience of the world's seagrass meadows. J. Appl. Ecol. 53, 967–972.
Duffy, J.E., Benedetti-Cecchi, L., Trinanes, J., Muller-Karger, F.E., Ambo-Rappe, R., Boström, C., et al., 2019. Toward a coordinated global observing system for seagrasses and marine macroalgae. Front. Mar. Sci. 6, 317.

Feng, S.F., Huang, X.P., Zhang, J.P., 2013. Subcellular distribution of cadmium in seagrass *Thalassia hemprichii* and its ecological significance under coupled stress of copper and cadmium. Mar. environ. Sci. 32 (3), 1545–1550 (In Chinese).
Firth, D.C., Salie, K., O'Neill, B., Hoffman, L.C., 2019. Monitoring of trace metal accumulation in two South African farmed mussel species, *Mytilus galloprovincialis* and *Choromytilus meridionalis*. Mar. Pollut. Bull. 141, 529–534.
Fourqurean, J.W., Duarte, C.M., Kennedy, H., Marba, N., Holmer, M., Mateo, M.A., Apostolaki, E.T., Kendrick, G.A., Krause-Jensen, D., McGlathery, K.J., Serrano, O., 2012. Seagrass ecosystems as a globally significant carbon stock. Nat. Geosci. 5, 505–509.
Franssen, S.U., Gu, J., Winters, G., Huylmans, A.K., Wienpahl, I., Sparwel, M., Coyer, J. A., Olsen, J.L., Reusch, T.B., Bornberg-Bauer, E., 2014. Genome-wide transcriptomic responses of the seagrasses *Zostera marina* and *Nanozostera noltii* under a simulated heatwave confirm functional types. Mar. Genom. 15, 65–73.
Franzle, O., 2006. Complex bioindication and environmental stress assessment. Ecol. Indic. 6, 114–136.
Fu, X.P., Dou, C.M., Chen, Y.X., Chen, X.C., Shi, J.Y., Yu, M.G., Xu, J., 2011. Subcellular distribution and chemical forms of cadmium in *Phytolacca americana* L. J. Hazard. Mater. 186, 103–107.
Gallego, S.M., Pena, L.B., Barcia, R.A., Azpilicueta, C.E., Lannone, M.F., Rosales, E.P., Zawoznik, M.S., Groppa, M.D., Benavides, M.P., 2012. Unravelling cadmium toxicity and tolerance in plants: insight into regulatory mechanisms. Environ. Exp. Bot. 83, 33–46.
Gillanders, B.M., 2007. Seagrasses, Fish, and fisheries. Seagrasses: Biology, Ecology and Conservation. Springer, Dordrecht.
Govers, L.L., van der Zee, E.M., Meffert, J.P., van Rijswick, P.C., Man In't Veld, W.A., Heusinkveld, J.H., van der Heide, T., 2017. Copper treatment during storage reduces *Phytophthora* and *Halophytophthora* infection of *Zostera marina* seeds used for restoration. Sci. Rep. 7, 43172.
Grabherr, M.G., Haas, B.J., Yassour, M., Levin, J.Z., Thompson, D.A., Amit, I., Adiconis, X., Fan, L., Raychowdhury, R., Zeng, Q.D., Chen, Z.H., Mauceli, E., Hacohen, N., Gnirke, A., Rhind, N., di Palma, F., Birren, B.W., Nusbaum, C., Lindblad-Toh, K., Friedman, N., Regev, A., 2011. Full-length transcriptome assembly from RNA-Seq data without a reference genome. Nat. Biotechnol. 29, 644–U130.
Greco, M., Chiappetta, A., Bruno, L., Bitonti, M.B., 2012. In *Posidonia oceanica* cadmium induces changes in DNA methylation and chromatin patterning. J. Exp. Bot. 63, 695–709.
Greco, M., Saez, C.A., Contreras, R.A., Rodriguez-Rojas, F., Bitonti, M.B., Brown, M.T., 2019. Cadmium and/or copper excess induce interdependent metal accumulation, DNA methylation, induction of metal chelators and antioxidant defences in the seagrass *Zostera marina*. Chemosphere 224, 111–119.
Gu, R.T., Zhou, Y., Song, X.Y., Xu, S.C., Zhang, X.M., Lin, H.Y., Xu, S., Zhu, S.Y., 2018. Effects of temperature and salinity on *Ruppia sinensis* seed germination, seedling establishment, and seedling growth. Mar. Pollut. Bull. 134, 177–185.
Gu, R.T., Zhou, Y., Song, X.Y., Xu, S.C., Zhang, X.M., Lin, H.Y., Xu, S., Yue, S.D., Zhu, S. Y., 2018. Tolerance of *Ruppia sinensis* seeds to desiccation, low temperature, and high salinity with special reference to long-term seed storage. Front. Plant Sci. 9, 221.
Gu, R.T., Song, X.Y., Zhou, Y., Zhang, X.M., Xu, S.C., Xu, S., Yue, S.D., Zhang, Y., Zhu, S. Y., 2019. *In situ* investigation of the influence of desiccation on sediment seed banks and population recruitment of the seagrass *Ruppia sinensis* in the Yellow River Delta, China. Mar. Pollut. Bull. 149, 110620.
Hamoutene, D., Romeo, M., Gnassia, M., Lafaurie, M., 1996. Cadmium effects on oxidative metabolism in a marine seagrass: *Posidonia oceanica*. B. Environ. Contam. Tox. 56, 327–334.
He, J., Li, H., Luo, J., Ma, C., Li, S., Qu, L., Gai, Y., Jiang, X., Janz, D., Polle, A., Tyree, M., Luo, Z.B., 2013. A transcriptomic network underlies microstructural and physiological responses to cadmium in *Populus* x *canescens*. Plant Physiol. 162, 424–439.
Hu, C., Yang, X., Gao, L., Zhang, P., Li, W., Dong, J., Li, C., Zhang, X., 2019. Comparative analysis of heavy metal accumulation and bioindication in three seagrasses: which species is more suitable as a bioindicator? Sci.Total Environ. 669, 41–48.
Huybrechts, M., Cuypers, A., Deckers, J., Iven, V., Vandionant, S., Jozefczak, M., Hendrix, S., 2019. Cadmium and plant development: an agony from seed to seed. Int. J. Mol. Sci. 20 (16), 3971.
Jacob, C., Buffard, A., Pioch, S., Thorin, S., 2018. Marine ecosystem restoration and biodiversity offset. Ecol. Eng. 120, 585–594.
Jayathilake, D.R.M., Costello, M.J., 2018. A modelled global distribution of the seagrass biome. Biol. Conserv. 226, 120–126.
Kanehisa, M., Araki, M., Goto, S., et al., 2008. KEGG for linking genomes to life and the environment. Nucleic Acids Res. 36, D480–D484.
Kendrick, G.A., Nowicki, R.J., Olsen, Y.S., Strydom, S., Fraser, M.W., Sinclair, E.A., et al., 2019. A systematic review of how multiple stressors from an extreme event drove ecosystem-wide loss of resilience in an iconic seagrass community. Front. Mar. Sci. 6, 455.
Kilminster, K., 2013. Trace element content of seagrasses in the Leschenault Estuary, Western Australia. Mar. Pollut. Bull. 73, 381–388.
Körpe, D.A., Aras, S., 2011. Evaluation of copper-induced stress on eggplant (*Solanum melongena* L.) seedlings at the molecular and population levels by use of various biomarkers. Mutat. Res.-Gen.Tox. En. 719, 29–34.
Lee, S.Y., Kim, J.B., Lee, S.M., 2006. Temporal dynamics of subtidal *Zostera marina* and intertidal *Zostera japonica* on the southern coast of Korea. Mar. Ecol. Evol. Persp. 27, 133–144.
Lee, G., Suonan, Z., Kim, S.H., Hwang, D.W., Lee, K.S., 2019. Heavy metal accumulation and phytoremediation potential by transplants of the seagrass *Zostera marina* in the polluted bay systems. Mar. Pollut. Bull. 149, 110509.
Lefcheck, J.S., Wilcox, D.J., Murphy, R.R., Marion, S.R., Orth, R.J., 2017. Multiple stressors threaten the imperiled coastal foundation species eelgrass (*Zostera marina*) in Chesapeake Bay, USA. Glob. Change Biol. 23, 3474–3483.
Li, B., Dewey, C.N., 2011. RSEM: accurate transcript quantification from RNA-Seq data with or without a reference genome. BMC Bioinformatics 12, 323.
Lin, H.Y., Sun, T., Zhou, Y., Zhang, X.M., 2016. Anti-oxidative feedback and biomarkers in the intertidal seagrass *Zostera japonica* caused by exposure to copper, lead and cadmium. Mar. Pollut. Bull. 109, 325–333.
Lin, H.Y., Sun, T., Zhou, Y., Gu, R.T., Zhang, X.M., Yang, W., 2018. Which genes in a typical intertidal seagrass (*Zostera japonica*) indicate Copper-, Lead-, and Cadmium pollution? Front. Plant Sci. 9, 1545.
Liu, X.J., Zhou, Y., Yang, H.S., Ru, S.G., 2013. Eelgrass detritus as a food source for the sea cucumber *Apostichopus japonicus* Selenka (Echinidermata: Holothuroidea) in coastal waters of North China: an experimental study in flow-through systems. PLoS One 8, e58293.
Liu, J., Cao, L., Dou, S., 2019. Trophic transfer, biomagnification and risk assessments of four common heavy metals in the food web of Laizhou Bay, the Bohai Sea. Sci. Total Environ. 670, 508–522.
Liu, H.J., Yang, L., Li, N., Zhou, C.J., et al., 2020. Cadmium toxicity reduction in rice (*Oryza sativa* L.) through iron addition during primary reaction of photosynthesis. Ecotoxicol. Environ. Saf. 200, 110746.
Livak, K.J., Schmittgen, T.D., 2001. Analysis of relative gene expression data using real-time quantitative PCR and the $2^{-\Delta\Delta C_T}$ method. Methods 25, 402–408.
Lodish, H., Berk, A., Zipursky, S.L., Matsudaira, P., Baltimore, D., Darnell, J., 2000. Biomembranes: structural organization and basic functions. Molecular Cell Biology, 4th edition. WH Freeman.
Lux, A., Martinka, M., Vaculík, M., White, P.J., 2011. Root responses to cadmium in the rhizosphere: a review. J. Exp. Bot. 62, 21–37.
Lyngby, J.E., Brix, H., 1982. Seasonal and environmental variation in cadmium, copper, lead and zinc concentrations in eelgrass (*Zostera marina* L.) in the limfjord, Denmark. Aquat. Bot. 14, 59–74.
Malea, P., Boubonari, T., Kevrekidis, T., 2008. Iron, zinc, copper, lead and cadmium contents in *Ruppia maritima* from a Mediterranean coastal lagoon: monthly variation and distribution in different plant fractions. Bot. Mar. 51, 320–330.
Malea, P., Kevrekidis, T., Mogias, A., Adamakis, I.D.S., 2014. Kinetics of cadmium accumulation and occurrence of dead cells in leaves of the submerged angiosperm Ruppia maritima. Bot. Mar. 57, 111–122.
Marion, S.R., Orth, R.J., 2010. Innovative techniques for large-scale seagrassrestoration using *Zostera marina* (eelgrass) seeds. Restor. Ecol. 18, 514–526.
Martínez-Crego, B., Vergés, A., Alcoverro, T., Romero, J., 2008. Selection of multiple seagrass indicators for environmental biomonitoring. Mar. Ecol. Prog. Ser. 361, 93–109.
Maxwell, P.S., Eklof, J.S., van Katwijk, M.M., O'Brien, K.R., de la Torre-Castro, M., Bostrom, C., Bouma, T.J., Krause-Jensen, D., Unsworth, R.K.F., van Tussenbroek, B. I., 2017. The fundamental role of ecological feedback mechanisms for the adaptive management of seagrass ecosystems - a review. Biol. Rev. 92, 1521–1538.
Mohammadi, N.S., Buapet, P., Pernice, M., Signal, B., Kahlke, T., Hardke, L., Ralph, P.J., 2019. Transcriptome profiling analysis of the seagrass, *Zostera muelleri* under copper stress. Mar. Pollut. Bull. 149, 110556.
Nouri, J., Khorasani, N., Lorestani, B., Karami, M., Hassani, A.H., Yousefi, N., 2009. Accumulation of heavy metals in soil and uptake by plant species with phytoremediation potential. Environ. Earth Sci. 59, 315–323.
Orth, R.J., Carruthers, T.J.B., Dennison, W.C., Duarte, C.M., Fourqurean, J.W., Heck, K. L., Hughes, A.R., Kendrick, G.A., Kenworthy, W.J., Olyarnik, S., Short, F.T., Waycott, M., Williams, S.L., 2006. A global crisis for seagrass ecosystems. BioScience 56, 987–996.
Paez-Garcia, A., Sparks, J.A., de Bang, L., Blancaflor, E.B., 2018. Plant actin cytoskeleton: new functions from Old scaffold. In: Sahi, V., Baluška, F. (Eds.), Concepts in Cell Biology - History and Evolution. Plant Cell Monographs, vol 23. Springer, Cham.
Pan, K., Wang, W.X., 2012. Trace metal contamination in estuarine and coastal environments in China. Sci. Total Environ. 421, 3–16.
Park, J., Song, W.Y., Ko, D., Eom, Y., Hansen, T.H., Schiller, M., Lee, T.G., Martinoia, E., Lee, Y., 2012. The phytochelatin transporters AtABCC1 and AtABCC2 mediate tolerance to cadmium and mercury. Plant J. 69, 278–288.
Perea-Juarez, R.N., Frias-Espericueta, M.G., Paez-Osuna, F., Voltolina, D., 2016. Copper, zinc, cadmium and lead inputs and outputs in the maternity section of a commercial shrimp hatchery. Lat. Am. J. Aquat. Res. 44, 595–601.
Pittman, J.K., 2005. Managing the manganese: molecular mechanisms of manganese transport and homeostasis. New Phytol. 167, 733–742.
Qin, Y., Dong, J., 2015. Focusing on the focus: what else beyond the master switches for polar cell growth? Mol. Plant 8, 582–594.
Ralph, P.J., Burchett, M.D., 1998. Photosynthetic response of *Halophila ovalis* to heavy metal stress. Environ. Pollut. 103, 91–101.
Reynolds, L.K., Waycott, M., McGlathery, K.J., 2013. Restoration recovers population structure and landscape genetic connectivity in a dispersal-limited ecosystem. J. Ecol. 101, 1288–1297.
Roberts, D.A., Johnston, E.L., Poore, A.G.B., 2008. Contamination of marine biogenic habitats and effects upon associated epifauna. Mar. Pollut. Bull. 56, 1057–1065.
Sabiha-Javied, Mehmood, T., Chaudhry, M.M., Tufail, M., Irfan, N., 2009. Heavy metal pollution from phosphate rock used for the production of fertilizer in Pakistan. Microchem. J. 91, 94–99.
Sanchez-Quiles, D., Marba, N., Tovar-Santhez, A., 2017. Trace metal accumulation in marine macrophytes: hotspots of coastal contamination worldwide. Sci. Total Environ. 576, 520–527.

Sanchiz, C., Garcia-Carrascosa, A.M., Pastor, A., 1999. Bioaccumulation of Hg, Cd, Pb and Zn in four marine phanerogams and the alga *Caulerpa prolifera* (forsskal) lamouroux from the east coast of Spain. Bot. Mar. 42, 157–164.

Sharma, S.S., Dietz, K.J., Mimura, T., 2016. Vacuolar compartmentalization as indispensable component of heavy metal detoxification in plants. Plant Cell Environ. 39, 1112–1126.

Shi, W., Zhang, Y., Chen, S., Polle, A., Rennenberg, H., Luo, Z.B., 2019. Physiological and molecular mechanisms of heavy metal accumulation in nonmycorrhizal versus mycorrhizal plants. Plant Cell Environ. 42 (4), 1087–1103.

Short, F.T., Polidoro, Livingstone, B., Carpenter, S.R., Bandeira, K.E., Bujang, S., Calumpong, J.S., H.P, Carruthers, T.J.B., Coles, R.G., Dennison, W.C., Erftemeijer, P. L.A., Fortes, M.D., Freeman, A.S., Jagtap, T.G., Kamal, A.H.M., Kendrick, G.A., Kenworthy, W.J., La Nafie, Y.A., Nasution, I.M., Orth, R.J., Prathep, A., Sanciangco, J.C., Tussenbroek, Bv., Vergara, S.G., Waycott, M., Zieman, J.C., 2011. Extinction risk assessment of the world's seagrass species. Biol. Conserv. 144, 1961–1971.

Statton, J., Montoya, L.R., Orth, R.J., Dixon, K.W., Kendrick, G.A., 2017. Identifying critical recruitment bottlenecks limiting seedling establishment in a degraded seagrass ecosystem. Sci. Rep. 7, 14786.

Tada, K., Yamaguchi, H., Montani, S., 2004. Comparison of chlorophyll *a* concentrations obtained with 90% acetone and N, N-dimethylformamide extraction in coastal seawater. J. Oceanogr. 60, 259–261.

Taylor, M.D., Fry, B., Becker, A., Moltschaniwskyj, N., 2017. Recruitment and connectivity influence the role of seagrass as a penaeid nursery habitat in a wave dominated estuary. Sci.Total Environ. 58, 622–630.

Thomsen, S., Anders, S., Janga, S.C., Huber, W., Alonso, C.R., 2010. Genome-wide analysis of mRNA decay patterns during early Drosophila development. Genome Biol. 11, R93.

Thounaojam, T.C., Panda, P., Mazumdar, P., Kumar, D., Sharma, G.D., Sahoo, L., Sanjib, P., 2012. Excess copper induced oxidative stress and response of antioxidants in rice. Plant Physiol. Biochem. 53, 33–39.

Tian, K., Wu, Q., Liu, P., Hu, W., Huang, B., Shi, B., Zhou, Y., Kwon, B.O., Choi, K., Ryu, J., Seong Khim, J., Wang, T., 2020. Ecological risk assessment of heavy metals in sediments and water from the coastal areas of the Bohai Sea and the Yellow Sea. Environ. Int. 136, 105512.

Trapnell, C., Williams, B.A., Pertea, G., Mortazavi, A., Kwan, G., van Baren, M.J., Salzberg, S.L., Wold, B.J., Pachter, L., 2010. Transcript assembly and quantification by RNA-Seq reveals unannotated transcripts and isoform switching during cell differentiation. Nat. Biotechnol. 28, 511–U174.

Unsworth, R.K.F., Nordlund, L.M., Cullen-Unsworth, L.C., 2018. Seagrass meadows support global fisheries production. Conserv. Lett. e12566.

van Katwijk, M.M., Thorhaug, A., Marbà, N., Orth, R.J., Duarte, C.M., Kendrick, G.A., et al., 2016. Global analysis of seagrass restoration: the importance of large-scale planting. J. Appl. Ecol. 53, 567–578.

Verhoeven, J.T.A., 1979. Ecology of *ruppia*-dominated communities in Western-Europe. 1. Distribution of *Ruppia* representatives in relation to their autecology. Aquat. Bot. 6, 197–268.

Wang, Q.Y., Liu, J.S., Hu, B., 2016. Integration of copper subcellular distribution and chemical forms to understand copper toxicity in apple trees. Environ. Exp. Bot. 123, 125–131.

Waycott, M., Duarte, C.M., Carruthers, T.J.B., Orth, R.J., Dennison, W.C., Olyarnik, S., Calladine, A., Fourqurean, J.W., Heck, K.L., Hughes, A.R., Kendrick, G.A., Kenworthy, W.J., Short, F.T., Williams, S.L., 2009. Accelerating loss of seagrasses across the globe threatens coastal ecosystems. Proc. Natl. Acad. Sci. U. S. A. 106, 12377–12381.

Welschmeyer, N.A., 1994. Fluorometric analysis of chlorophyll-a in the presence of chlorophyll-B and pheopigments. Limnol. Oceanogr. 39, 1985–1992.

Wu, F.B., Dong, J., Qian, Q.Q., Zhang, G.P., 2005. Subcellular distribution and chemical form of Cd and Cd-Zn interaction in different barley genotypes. Chemosphere 60, 1437–1446.

Xu, S.C., Zhou, Y., Wang, P.M., Wang, F., Zhang, X.M., Gu, R.T., 2016. Salinity and temperature significantly influence seed germination, seedling establishment, and seedling growth of eelgrass *Zostera marina* L. PeerJ 4, e2697.

Xu, S.C., Wang, P.M., Zhou, Y., Zhang, X.M., Gu, R.T., Liu, X.J., Yue, S.D., 2018. New insights into different reproductive effort and sexual recruitment contribution between two geographic *Zostera marina* L. populations in temperate China. Front. Plant Sci. 9, 15.

Young, M.D., Wakefield, M.J., Smyth, G.K., Oshlack, A., 2010. Gene ontology analysis for RNA-seq: accounting for selection bias. Genome Biol. 11, R14.

Yu, S., den Hartog, C., 2014. Taxonomy of the genus *Ruppia* in China. Aquat. Bot. 119, 66–72.

Yue, S.D., Zhou, Y., Zhang, Y., Xu, S.C., Gu, R.T., Xu, S., Zhang, X.M., 2019. Effects of salinity and temperature on seed germination and seedling establishment in the endangered seagrass *Zostera japonica* Asch. & Graebn. in northern China. Mar. Pollut. Bull. 146, 848–856.

Zhang, M., He, P., Qiao, G., Huang, J., Yuan, X., Li, Q., 2019. Heavy metal contamination assessment of surface sediments of the Subei Shoal, China: spatial distribution, source apportionment and ecological risk. Chemosphere 223, 211–222.

Zheng, J., Gu, X.Q., Zhang, T.J., Liu, H.H., Ou, Q.J., Peng, C.L., 2018. Phytotoxic effects of Cu, Cd and Zn on the seagrass *Thalassia hemprichii* and metal accumulation in plants growing in Xincun Bay, Hainan, China. Ecotoxicology 27, 517–526.

Zhou, Y., Liu, P., Liu, B.J., Liu, X.J., Zhang, X.M., Wang, F., Yang, H.S., 2014. Restoring eelgrass (*Zostera marina* L.) habitats using a simple and effective transplanting technique. PLoS One 9, e92982.

Zimeri, A.M., Dhankher, O.P., McCaig, B., Meagher, R.B., 2005. The plant MT1 metallothioneins are stabilized by binding cadmiums and are required for cadmium tolerance and accumulation. Plant Mol. Biol. 58, 839–855.